

POD Reduced-order Model for Aeroacoustic Applications

Original

POD Reduced-order Model for Aeroacoustic Applications / Arina, Renzo. - ELETTRONICO. - (2017). (AIAA Aviation Forum Denver, Colorado, USA 5-9 June 2017).

Availability:

This version is available at: 11583/2701833 since: 2023-07-01T09:32:19Z

Publisher:

AIAA

Published

DOI:

Terms of use:

This article is made available under terms and conditions as specified in the corresponding bibliographic description in the repository

Publisher copyright

(Article begins on next page)



POD Reduced-Order Model for Aeroacoustic Applications

Renzo Arina*

Dipartimento di Ingegneria Meccanica e Aerospaziale, Politecnico di Torino, Torino, 10129, Italy

A reduced-order model (ROM) for acoustic propagation is proposed. It is based on a Proper Orthogonal Decomposition (POD) of a set of snapshots, obtained for different values of geometrical and frequency parameters of the acoustic problem under study. The POD expansion coefficients, functions of the parameters, are continuously extended in the parameter space by interpolation. This approach is termed POD with Interpolation (PODI). The model is applied to the case of the scattering of sound by a circular cylinder. The problem is formulated in the frequency space and the parameter is the distance of the monopole source with respect to the circular cylinder. It is shown that the proposed methodology is able to correctly capture the main features of the acoustic field, such as the SPL field.

I. Introduction

Recent years have seen considerable progress in solution methods for Linearized Euler equations (LEE) and Linearized Navier-Stokes equations (LNSE) in aeroacoustics,^{1,2} leading to advances across a broad range of engineering applications. Improvements in methodology, together with a substantial increase in computing power, are such that real-time simulation and optimization of systems governed by LEEs, or LNSEs, is now an attainable goal. In many cases, computational models for such applications yield very large systems that are computationally intensive to solve. A critical element towards achieving a real-time simulation capability is the development of accurate, efficient models that can be rapidly solved.

Model reduction is a powerful tool that allows the systematic generation of cost-efficient representations of large-scale systems resulting from discretization of LEEs/LNSEs. Reduction methodology has been developed and applied for many different disciplines, including controls, fluid dynamics, structural dynamics, and circuit design. Considerable advances in the field of model reduction for large-scale systems have been made and many different applications have been demonstrated with success.³ To our knowledge no systematic study of model reduction has been presented in aeroacoustics yet, addressing a number of important issues, including the reliability of reduction techniques, associated with the quality of the reduced models, and validity of the model over a range of operating conditions.

Different model reduction techniques have been proposed.³ In this paper the attention is focused on the Proper Orthogonal Decomposition (POD), a general technique for extracting the most significant characteristics of a system and representing them in a set of POD low-dimensional basis vectors. The POD basis provide a low-dimensional description of the system in which to perform parametric interpolation. POD reduced models are derived and used with an offline-online strategy. The offline phase involves expensive high-fidelity simulations to generate the snapshots needed to compute the POD basis and to derive the Reduced-Order Model (ROM). In the online phase the ROM is used to achieve rapid computations.

In fluid dynamics, the POD is usually employed to find a basis for the projection of the Navier-Stokes equations and to obtain a ROM composed by a system of ordinary differential equations for the time dependent POD expansion coefficients.⁴ Less commonly, the POD is applied in the frequency space⁵ or in a parameter space. In this latter case, as an example, the POD can be used to describe flow fields around modified body shapes, using the information about the flow past few selected geometries of the body, which form the snapshots for the POD. Examples of this approach can be found in the works of Legresley and Alonso,⁶ Bui-Thanh et al.,⁷ Mifsud et al.⁸ and Tang and Shyy.⁹

*Professor, Dipartimento di Ingegneria Meccanica e Aerospaziale, renzo.arina@polito.it, AIAA Senior Member

The application of POD-based ROMs in the parameter space is quite recent and still under active development. Moreover, to our knowledge, no systematic study of model reduction has been presented in aeroacoustics yet, addressing a number of important issues, including the reliability of reduction techniques, associated with the quality of the reduced models, and validity of the model over a range of operating conditions.

In the next Section the general frame of the reduced-order projection is presented. The POD method is described in detail in Section 3 and in Section 4 it is applied to the problem of the scattering of sound by a circular cylinder. The problem is formulated in the frequency space and the parameter is the distance of the monopole source with respect to the circular cylinder.

II. Problem Statement and Reduced-Order Projection

The system of PDEs, governing acoustic propagation, can be discretized in the spatial domain using a numerical formulation (e.g. Discontinuous Galerkin method¹⁰) to yield a set of linear ordinary differential equations. As general form, the linear system can be written as

$$\mathbf{E} \frac{d\mathbf{u}(t)}{dt} + \mathbf{A}\mathbf{u}(t) = \mathbf{B}\boldsymbol{\mu}(t), \quad (1)$$

where $\mathbf{u}(t) \in \mathbb{R}^n$ is the state vector of the unknown acoustic flow quantities $(\rho', \rho' \mathbf{u}', p')$ at each point in the computational grid. $\mathbf{A} \in \mathbb{R}^{n \times n}$ and $\mathbf{E} \in \mathbb{R}^{n \times n}$ are the model operators. $\boldsymbol{\mu} \in \mathbb{R}^p$ is a vector of p parameters and $\mathbf{B} \in \mathbb{R}^{n \times p}$ is the input forcing operator. In general, particular output quantities are of interest, defining the vector $\mathbf{y} \in \mathbb{R}^q$ to be the q output quantities we have, with $\mathbf{C} \in \mathbb{R}^{q \times n}$,

$$\mathbf{y}(t) = \mathbf{C}\mathbf{u}(t), \quad (2)$$

Vectors $\boldsymbol{\mu}(t)$ and $\mathbf{y}(t)$ in problem (1) and (2) contain the system inputs and outputs respectively. The definition of inputs and outputs will depend upon the specific problem under exam. For example inputs may consist of specif noise sources or body motion, while outputs of interest may be the generated sound pressure level (SPL). For active control applications, the output might monitor an acoustic condition at a particular location while inputs describe both actuation mechanisms and acoustic source disturbances.

Considering a harmonic forcing $\boldsymbol{\mu} = \hat{\boldsymbol{\mu}}e^{i\omega t}$, problem (1) and (2) can be formulated in the frequency domain

$$G : (i\omega\mathbf{E} + \mathbf{A}) \hat{\mathbf{u}} = \mathbf{B}\hat{\boldsymbol{\mu}}, \quad \hat{\mathbf{y}} = \mathbf{C}\hat{\mathbf{u}}, \quad (3)$$

where $\mathbf{u} = \hat{\mathbf{u}}e^{i\omega t}$ and $\mathbf{y} = \hat{\mathbf{y}}e^{i\omega t}$.

Matrices \mathbf{A} , \mathbf{C} , and \mathbf{E} in the problem (3) are defined by the mean flow conditions. In comparison with nonlinear problems, system (3) is relatively efficient. However, the order n of the system is still prohibitively high for many applications, and the cost to solve the system can be too large for implementation in real time. Therefore it is interesting to find a low-order linear reduced model

$$\tilde{G} : (i\omega\tilde{\mathbf{E}} + \tilde{\mathbf{A}}) \tilde{\mathbf{u}} = \tilde{\mathbf{B}}\hat{\boldsymbol{\mu}}, \quad \tilde{\mathbf{y}} = \tilde{\mathbf{C}}\tilde{\mathbf{u}}, \quad (4)$$

which approximates well the given stable model (3). Typically, \mathbf{A} in system (3) is a sparse, square matrix of very large dimensions $n > 10^5$, and the desired order m of \tilde{G} can be less than 50. The quality of \tilde{G} as an approximation of G is defined as the H_∞ norm of the difference between their transfer functions $\|\hat{G} - G\|$ which in turn equals the square root of the maximal energy of the difference $e = \hat{\mathbf{y}} - \mathbf{y}$, given by $\|\hat{\mathbf{y}} - \mathbf{y}\|^2$.

The reduced model is obtained projecting the problem onto a reduced space defined of few basis vectors. The full state vector $\hat{\mathbf{u}}$ is represented in a reduced-space basis

$$\hat{\mathbf{u}} = \mathbf{U}\tilde{\mathbf{u}}, \quad (5)$$

where the columns of the matrix $\mathbf{U} \in \mathbb{R}^{n \times m}$ contain m basis vectors. Defining a left projection space \mathbf{V} so that $\mathbf{W}^T \mathbf{U} = \mathbf{I}$, the governing equations (3) can be projected onto the reduced space to yield an m^{th} -order model of the form

$$\tilde{G} : [i\omega(\mathbf{W}^T \mathbf{E} \mathbf{U}) + (\mathbf{W}^T \mathbf{A} \mathbf{U})] \tilde{\mathbf{u}} = (\mathbf{W}^T \mathbf{B}) \hat{\boldsymbol{\mu}}, \quad \hat{\mathbf{y}} = (\mathbf{C} \mathbf{U}) \tilde{\mathbf{u}}.$$

Therefore $\tilde{\mathbf{E}} \equiv \mathbf{W}^T \mathbf{E} \mathbf{U} \in \mathbb{R}^{m \times m}$, $\tilde{\mathbf{A}} \equiv \mathbf{W}^T \mathbf{A} \mathbf{U} \in \mathbb{R}^{m \times m}$, $\tilde{\mathbf{B}} \equiv \mathbf{W}^T \mathbf{B} \in \mathbb{R}^{m \times p}$ and $\tilde{\mathbf{C}} \equiv \mathbf{W}^T \mathbf{C} \in \mathbb{R}^{q \times m}$.

The reduction task is to find a suitable basis \mathbf{U} so that $m \ll n$ and the reduction error e is small. Accuracy of reduced models is an important issue for which a rigorous analysis is necessary. Amongst the several existing methods for computing the basis, the POD projection method provide an accuracy analysis.

III. Proper Orthogonal Decomposition and Model Order Reduction

POD was introduced by Lumley^{11,12} for the analysis of the structures of turbulent flows. It is closely related to the Karhunen-Loève decomposition¹³ of stochastic processes, the principal component analysis¹⁴ in statistical analysis and the Singular Value Decomposition (SVD). It can be shown that they are all equivalent.¹⁵

POD basis vectors are computed using a set of data called *snapshots*. Each snapshot is represented as a set of discrete data, a vector of dimension n , the number of grid points or cells times the number of unknown variables. The POD snapshots may be obtained from a simulation of the complete aeroacoustic model, the high-fidelity model, for different values of the p parameters. In the case of time dependent problems, the sampling can also be made selecting numerical solutions at constant time intervals¹⁶ or, in the case of frequency-space formulation, selecting a set of sample frequencies.¹⁷ The input choice is critical, since the resulting basis will capture only those dynamics present in the snapshot ensemble.

The POD described as a SVD problem¹⁸ is more straightforward for the present case, moreover it has the advantage of being more reliable than the eigenvalue decomposition for computing the smallest spectral information.

Once the set of POD basis has been computed, using time- or frequency-domain snapshots, the reduced-order model is obtained using the projection (5). It is important to note that, while the POD basis is optimal in the sense that it provides the most efficient representation of the data contained in the snapshot ensemble, one can make no statement regarding the quality of the resulting reduced-order model.

III.A. Singular Value Decomposition of a Real Matrix

Considering the rectangular matrix \mathbf{A} with columns $\mathbf{u}_j \in \mathbb{R}^n$, $1 \leq j \leq m$ representing m snapshots. m is the number of realizations obtained combining different values of the p parameters. Each snapshot corresponds to a vector of dimension n , solution of a high-fidelity calculation, where $n \gg m$. The SVD of the real valued matrix $\mathbf{A} = [\mathbf{u}_1, \dots, \mathbf{u}_m] \in \mathbb{R}^{n \times m}$, of rank m , guarantees the existence of m real numbers $\sigma_1 \geq \sigma_2 \geq \dots \geq \sigma_m > 0$ and of the orthonormal matrices $\mathbf{U} \in \mathbb{R}^{n \times n}$, with columns $\boldsymbol{\varphi}_i \in \mathbb{R}^n$, $1 \leq i \leq n$, and $\mathbf{V} \in \mathbb{R}^{m \times m}$, with columns $\boldsymbol{\psi}_j \in \mathbb{R}^m$, $1 \leq j \leq m$, such that

$$\mathbf{U}^T \mathbf{A} \mathbf{V} = \begin{pmatrix} \mathbf{D} \\ \mathbf{0} \end{pmatrix} \doteq \boldsymbol{\Sigma} \in \mathbb{R}^{n \times m}, \quad (6)$$

where $\mathbf{D} = \text{diag}(\sigma_1, \dots, \sigma_m) \in \mathbb{R}^{m \times m}$. Matrices \mathbf{U} and \mathbf{V} are orthonormal, that is $\mathbf{U}^T \mathbf{U} = \mathbf{U} \mathbf{U}^T = \mathbf{I}$, and $\mathbf{U}^T = \mathbf{U}^{-1}$. Similar relations hold for \mathbf{V} . Then, from (6), it follows

$$\mathbf{A} \mathbf{V} = \mathbf{U} \boldsymbol{\Sigma}, \quad (7)$$

and

$$\mathbf{A}^T \mathbf{U} = \mathbf{V} \boldsymbol{\Sigma}.$$

Moreover

$$\mathbf{A} = \mathbf{U} \boldsymbol{\Sigma} \mathbf{V}^T. \quad (8)$$

The diagonal matrix $\boldsymbol{\Sigma} \in \mathbb{R}^{n \times m}$ has m non-negative values, ordered in decreasing order, $\{\sigma_l\}_{l=1}^m$ which are the *singular values* of matrix \mathbf{A} . Vectors $\{\boldsymbol{\varphi}_i\}_{i=1}^n$ and $\{\boldsymbol{\psi}_j\}_{j=1}^m$ are respectively the *left* and *right singular vectors* of matrix \mathbf{A} .

From (8) it follows

$$\mathbf{A}^T = \left(\mathbf{U} \boldsymbol{\Sigma} \mathbf{V}^T \right)^T = \mathbf{V} (\mathbf{U} \boldsymbol{\Sigma})^T = \mathbf{V} \boldsymbol{\Sigma} \mathbf{U}^T,$$

and

$$(\mathbf{A}^T \mathbf{A}) \mathbf{V} = \left(\mathbf{V} \boldsymbol{\Sigma} \mathbf{U}^T \mathbf{U} \boldsymbol{\Sigma} \mathbf{V}^T \right) \mathbf{V} = \mathbf{V} \boldsymbol{\Sigma}^2 \mathbf{V}^T \mathbf{V} = \mathbf{V} \boldsymbol{\Sigma}^2 = \mathbf{A} \mathbf{V}, \quad (9)$$

setting $\mathbf{\Lambda} = \mathbf{\Sigma}^2$, the diagonal matrix with elements $\lambda_l = \sigma_l^2 > 0$ ($1 \leq l \leq m$), vectors $\{\psi_l\}_{l=1}^m$ are the eigenvectors of the matrix $\mathbf{A}^T \mathbf{A}$ with eigenvalues λ_l . Similarly

$$(\mathbf{A} \mathbf{A}^T) \mathbf{U} = (\mathbf{U} \mathbf{\Sigma} \mathbf{V}^T \mathbf{V} \mathbf{\Sigma} \mathbf{U}^T) \mathbf{U} = \mathbf{\Sigma}^2 \mathbf{U} = \mathbf{\Lambda} \mathbf{U}, \quad (10)$$

vectors $\{\varphi_l\}_{l=1}^m$ are the eigenvectors of the matrix $\mathbf{A} \mathbf{A}^T$ with eigenvalues λ_l . The vectors $\{\varphi_l\}_{l=m+1}^n$ are eigenvectors with zero eigenvalue.

The column space of \mathbf{A} can be represented in terms of the linearly independent columns of \mathbf{U}

$$\mathbf{A} = \tilde{\mathbf{U}} \mathbf{D} \mathbf{V}^T = \tilde{\mathbf{U}} \mathbf{B},$$

with $\tilde{\mathbf{U}} \in \mathbb{R}^{n \times m}$ ($\tilde{U}_{ij} \equiv U_{ij}$ for $1 \leq i \leq n$, $1 \leq j \leq m$) and $\mathbf{B} = \mathbf{D} \mathbf{V}^T \in \mathbb{R}^{m \times m}$. Being $\tilde{\mathbf{U}}$ an orthogonal matrix ($\tilde{\mathbf{U}} \tilde{\mathbf{U}}^T = \mathbf{I} \in \mathbb{R}^{m \times m}$)

$$\begin{aligned} \mathbf{u}_j &= \sum_{l=1}^m B_{lj} \tilde{U}_{.l} = \sum_{l=1}^m (D \mathbf{V}^T)_{lj} \varphi_l = \sum_{l=1}^m (\tilde{U}^T \tilde{U} D \mathbf{V}^T)_{lj} \varphi_l \\ &= \sum_{l=1}^m (\tilde{U}^T \mathbf{A})_{lj} \varphi_l = \sum_{l=1}^m \langle \varphi_l, \mathbf{u}_j \rangle \varphi_l, \quad \text{for } j = 1, \dots, m, \end{aligned} \quad (11)$$

where $\langle \varphi_l, \mathbf{u}_j \rangle = \sum_{k=1}^n (\varphi_{kl} u_{kj})$ is the inner product in \mathbb{R}^n of the vectors $\varphi_l \in \mathbb{R}^n$ and $\mathbf{u}_j \in \mathbb{R}^n$.

III.B. SVD as Proper Orthogonal Decomposition

The central issue of the POD is to express the essential information of all snapshots $\{\mathbf{u}_j\}_{j=1}^m$ by means of a few basis vectors. The problem of approximating all snapshots simultaneously by a single, normalized, vector $\varphi \in \mathbb{R}^n$ as well as possible, can be expressed as

$$\max_{\varphi \in \mathbb{R}^n} \frac{1}{m} \sum_{j=1}^m |\langle \mathbf{u}_j, \varphi \rangle|^2 \quad \text{subject to} \quad \|\varphi\|^2 = 1, \quad (12)$$

where $\|\varphi\| = \sqrt{\langle \varphi, \varphi \rangle}$.

Considering the Lagrangian functional associated to (12),

$$\mathcal{L}(\varphi, \lambda) = \frac{1}{m} \sum_{j=1}^m |\langle \mathbf{u}_j, \varphi \rangle|^2 + \lambda (1 - \|\varphi\|^2) \quad \text{for } (\varphi, \lambda) \in \mathbb{R}^n \times \mathbb{R},$$

the function $\varphi \in \mathbb{R}^n$ is a solution to the constrained optimization problem (12), if the necessary condition

$$\nabla \mathcal{L}(\varphi, \lambda) = 0,$$

is satisfied. Computing the gradient of \mathcal{L} it follows, being $\mathbf{A} = [\mathbf{u}_1, \dots, \mathbf{u}_m]$,

$$\begin{aligned} \frac{\partial \mathcal{L}}{\partial \varphi_i}(\varphi, \lambda) &= \frac{\partial}{\partial \varphi_i} \left[\frac{1}{m} \sum_{j=1}^m \left| \sum_{k=1}^n A_{kj} \varphi_k \right|^2 + \lambda \left(1 - \sum_{k=1}^n \varphi_k^2 \right) \right] \\ &= \frac{2}{m} \sum_{j=1}^m \left(\sum_{k=1}^n A_{kj} \varphi_k \right) A_{ij} - 2\lambda \varphi_i = \frac{2}{m} \sum_{k=1}^n \sum_{j=1}^m A_{ij} A_{jk}^T \varphi_k - 2\lambda \varphi_i, \end{aligned}$$

we have

$$\nabla_{\varphi} \mathcal{L}(\varphi, \lambda) = 2 \left(\frac{1}{m} \mathbf{A} \mathbf{A}^T \varphi - \lambda \varphi \right) = 0 \quad \text{in } \mathbb{R}^n, \quad (13)$$

and

$$\frac{\partial \mathcal{L}}{\partial \lambda}(\varphi, \lambda) = 1 - \sum_{k=1}^n \varphi_k^2 = 1 - \|\varphi\|^2 = 0. \quad (14)$$

Conditions (13) and (14) lead to the eigenvalue problem for the symmetric matrix $\mathbf{A}\mathbf{A}^T$

$$\frac{1}{m}\mathbf{A}\mathbf{A}^T\boldsymbol{\varphi} = \lambda\boldsymbol{\varphi} \quad \text{in } \mathbb{R}^n, \quad (15)$$

with condition

$$\|\boldsymbol{\varphi}\| = 1. \quad (16)$$

The SVD of matrix \mathbf{A} shows that a vector $\boldsymbol{\varphi}_1$, solution of problem (15), is an eigenvector of $\mathbf{A}\mathbf{A}^T$ with eigenvalue $\lambda_1 = m\sigma_1^2 > 0$ [relation (10)]. It can be proved that $\boldsymbol{\varphi}_1$ satisfies the constrained optimization problem (12).¹⁸

Similarly, looking for a second vector $\boldsymbol{\varphi}_2$, orthogonal to $\boldsymbol{\varphi}_1$, describing the snapshots \mathbf{u}_j as well as possible, satisfying condition (12) and $\langle \boldsymbol{\varphi}_2, \boldsymbol{\varphi}_1 \rangle = 0$, SVD implies that $\boldsymbol{\varphi}_2$ is solution to the above constraint optimization problem and its argmax is equal to $\sigma_2^2 = m\lambda_2$. By finite induction the procedure can be continued.

The orthonormal vectors $\{\boldsymbol{\varphi}_i\}_{i=1}^l$ are called *POD basis of rank $l \leq m$* . The approximation of the snapshots $\{\mathbf{u}_j\}_{j=1}^m$, columns of \mathbf{A} , by the first l vectors $\{\boldsymbol{\varphi}_i\}_{i=1}^l$ is *optimal among all rank l approximations* to the columns of \mathbf{A} .¹⁸ The expansion of the columns of \mathbf{A} in the POD basis is given by, for (11) and $\tilde{\mathbf{U}} \in \mathbb{R}^{n \times l}$ being the matrix with columns formed by the POD basis $\{\boldsymbol{\varphi}_i\}_{i=1}^l$,

$$\mathbf{A} = \tilde{\mathbf{U}}\mathbf{B}^l \quad \text{where } B_{ij}^l = \langle \boldsymbol{\varphi}_i, \mathbf{u}_j \rangle \in \mathbb{R}^{l \times m} \quad \text{for } i \leq l, 1 \leq j \leq m. \quad (17)$$

The optimality of the POD basis implies that the POD basis of rank l satisfies the problem

$$\begin{aligned} \min_{\boldsymbol{\varphi}_1, \dots, \boldsymbol{\varphi}_l \in \mathbb{R}^n} \quad & \frac{1}{m} \sum_{j=1}^m \left\| \mathbf{u}_j - \sum_{i=1}^l \langle \mathbf{u}_j, \boldsymbol{\varphi}_i \rangle \boldsymbol{\varphi}_i \right\|^2 \\ \text{subject to } \quad & \langle \boldsymbol{\varphi}_i, \boldsymbol{\varphi}_j \rangle = \delta_{ij} \text{ for } 1 \leq i, j \leq l. \end{aligned}$$

A further property of the POD decomposition is that *the POD coefficients are uncorrelated*:

$$\begin{aligned} \sum_{j=1}^m B_{ij}^l B_{kj}^l &= \sum_{j=1}^m \langle \mathbf{u}_j, \boldsymbol{\varphi}_i \rangle \langle \mathbf{u}_j, \boldsymbol{\varphi}_k \rangle = \sum_{j=1}^m \langle \mathbf{u}_j, \boldsymbol{\varphi}_i \rangle \langle \mathbf{u}_j, \boldsymbol{\varphi}_k \rangle \\ &= \langle \sigma_i^2 \boldsymbol{\varphi}_i, \boldsymbol{\varphi}_k \rangle = \sigma_i^2 \delta_{ik}. \end{aligned}$$

To compute the POD basis of rank l , $\{\tilde{\boldsymbol{\varphi}}_i\}_{i=1}^l$, it is necessary to solve the $n \times n$ symmetric eigenvalue problem (15)

$$\frac{1}{m} (\mathbf{A}\mathbf{A}^T) \boldsymbol{\varphi}_i = \lambda_i \boldsymbol{\varphi}_i.$$

From relations (9) and (10) it follows $(\mathbf{A}^T \mathbf{A}) \mathbf{V} = (\mathbf{A}\mathbf{A}^T) \mathbf{U}$, therefore if $m < n$, it is more convenient to evaluate the eigenvectors $\boldsymbol{\psi}_1, \dots, \boldsymbol{\psi}_l \in \mathbb{R}^m$ solving the $m \times m$ symmetric eigenvalue problem (9)

$$\left(\frac{1}{m} \mathbf{A}^T \mathbf{A} \right) \boldsymbol{\psi}_i = \lambda_i \boldsymbol{\psi}_i \quad \text{for } i = 1, \dots, l,$$

matrix $\left(\frac{1}{m} \mathbf{A}^T \mathbf{A} \right)$ is the correlation matrix. And applying relation (7),

$$\mathbf{A}\boldsymbol{\psi}_i = \sigma_i \boldsymbol{\varphi}_i,$$

to obtain the POD basis

$$\boldsymbol{\varphi}_i = \frac{1}{\sigma_i} \mathbf{A}\boldsymbol{\psi}_i = \frac{1}{\sqrt{m\lambda_i}} \mathbf{A}\boldsymbol{\psi}_i \quad \text{for } i = 1, \dots, l. \quad (18)$$

This method is the so-called *method of snapshots*.¹⁹

The choice of l is of central importance for the POD. No a-priori rule is available, rather it is possible to apply an heuristic criterion based on the ratio of the modeled to the total energy contained in the system which can be expressed as

$$\varepsilon(l) = \frac{\sum_{i=1}^l \lambda_i}{\sum_{i=1}^m \lambda_i}. \quad (19)$$

III.C. Continuous Extension of the POD Projection Coefficients

The snapshot vector $\mathbf{u}_j \in \mathbb{R}^n$ represents a vector of scalar functions of grid points (or cells), such as the primitive variables of the acoustic field. The POD is applied to each variable to compute a distinct basis. As shown above [relation (17)], each snapshot \mathbf{u}_j can be expanded as,

$$\mathbf{u}_j = \sum_{l=1}^m \alpha_{lj} \boldsymbol{\varphi}_l \quad \text{for } j = 1, \dots, m,$$

with the projection coefficients

$$\alpha_{lj} = \langle \boldsymbol{\varphi}_l, \mathbf{u}_j \rangle.$$

The projection coefficients α_{lj} are discrete functions in the parameter space, with values defined at the points corresponding to the individual snapshots \mathbf{u}_j . To use the derived ROM as a prediction tool for a new configuration, it is necessary to extend the discrete functions α_{lj} as continuous functions α_l in the parameter space. In this way the field variable in a generic point of the parameter space may be approximated by the linear combination

$$\mathbf{u} = \sum_{l=1}^m \alpha_l \boldsymbol{\varphi}_l.$$

The combination of the POD and the continuous extension of the projection coefficients is termed POD with Interpolation (PODI).⁷

In the case of one-dimensional parameter spaces, the continuous extension can be obtained by linear or spline interpolation. For multidimensional spaces the method of the response surface can be adopted. The Response Surface Method (RSM) describes the continuous behaviour of a dependent variable by a set of simple basis functions.²⁰ Response surfaces are generally valid in a large region only in the case of few parameters; when a great number of parameters is involved, such as in the case of optimization problems, the RSM must be treated carefully. RSM has been originally developed for experimental data, employing regression techniques. In this way random experimental fluctuations are smoothed out. When the data set is provided by numerical simulations, a response surface obtained with a regression method in general does not fit exactly the data, introducing an undesirable smoothing. Therefore, other than a least square regression technique, interpolating methods, based on radial basis functions, can be employed.

IV. Numerical Example: Acoustic Scattering

The PODI-ROM method described in the previous section is applied to a problem of acoustic propagation in a homogeneous medium at rest, formulated in the frequency domain. The wave equation, in Cartesian coordinates and assuming the usual index summation convention,

$$\frac{1}{c_0^2} \frac{\partial^2 p'}{\partial t^2} - \delta_{ij} \frac{\partial^2 p'}{\partial x_i \partial x_j} = -Q_{ac}, \quad (20)$$

describes the propagation of sound through a homogeneous medium at rest. p' is the acoustic pressure, c_0 the sound speed evaluated at the medium conditions p_0 and ρ_0 , constant through the medium. $Q_{ac}(t, x_i)$ represents a source term (for example a line monopole source). Assuming harmonic time dependence for the acoustic fluctuations $p' = \hat{p} e^{i\omega t}$, Eq.(20) transforms in the complex Helmholtz equation

$$\delta_{ij} \frac{\partial^2 \hat{p}}{\partial x_i \partial x_j} + k^2 \hat{p} = \hat{Q}_{ac}, \quad (21)$$

with wave number $k = \omega/c_0$. The acoustic pressure can be computed after the inhomogeneous term Q_{ac} of Eq.(20) has been evaluated and Fourier transformed ($\hat{Q}_{ac}(k, x_i)$). In this way the range of the wave number $k \in [0, k_{max}]$ is introduced. For each value of k is associated the Helmholtz problem (21) with the corresponding inhomogeneous forcing term $\hat{Q}_{ac}(k, x_i)$. The time dependent acoustic pressure field is recovered performing an inverse DFT. Problem(21) is solved with a finite element method applying the code FreeFem++.²¹

The scattering of sound by a circular cylinder is a useful test for the validation of the PODI-ROM technique. Morris²² has provided the analytical solution of the scatter of sound from a monopole line source,

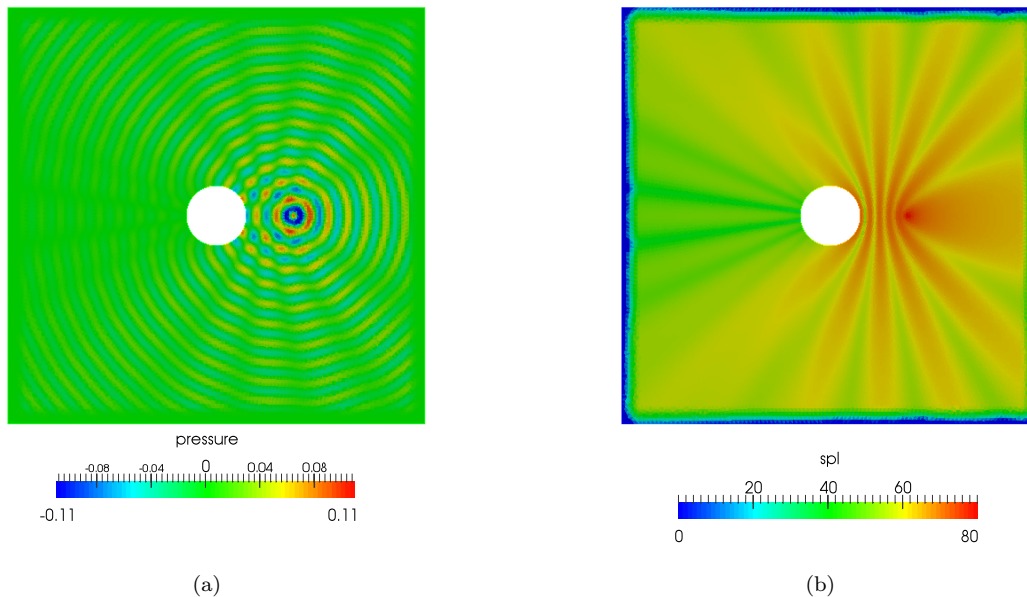


Figure 1. Scattering of a monopole acoustic source from a circular cylinder. $k = 10$. (a) Instantaneous pressure [Pa] and (b) SPL [dB].

positioned at a distance L , along the x -axis ($x_{source} = L, y_{source} = 0$), from a circular cylinder. The cylinder is centered in the origin of the axis, with ray R . The corresponding Helmholtz problem (21) has been solved on a square domain $[-2\pi : 2\pi] \times [-2\pi : 2\pi]$. To avoid spurious reflections along the exterior boundaries, Perfectly Matched Layer (PML) boundary conditions are imposed.²³ PML regions are added outside the exterior boundaries, and fully reflecting conditions ($\partial \hat{p} / \partial n = 0$) are imposed along the cylinder wall. The instantaneous acoustic pressure field is shown in Figure 1-(a) for the case of $k = 10$, corresponding to a frequency of 541.397 Hz, and $L/R = 2.5625$, and in Figure 1-(b) the SPL isocontours are displayed.

Keeping fixed the value of the wave number ($k = 10$), several snapshots are obtained varying the distance of the line source with respect to the cylinder center: L/R varying from 1.5 to 3.5. The high-fidelity calculations are performed on an unstructured grid of 36310 triangles. The numerical solutions coincide with the analytical solutions within round-off accuracy outside the source region.

As a first case, nine snapshots are obtained varying the distance L/R : 1.50, 1.75, 2.0, 2.25, 2.5, 2.75, 3.0, 3.25, 3.50. Once the POD coefficients α_{lj} , with $l = 1, 9$ and $j = 1, 9$, are obtained, the PODI-ROM is applied to reconstruct the solution for the case $k = 10$ and $L/R = 2.5625$. The POD coefficients are interpolated, with a parabolic interpolant, to obtain the values corresponding to the chosen parameter L/R .

In Figure 2-(a) the instantaneous pressure along the line $y = 0$ obtained with the high-fidelity (FEM) and the PODI-ROM reconstruction are compared. The interval $-1 \leq L/R \leq 1$ corresponds to the interior of the cylinder. In the *rear* part of the cylinder, with respect to the source, the weak pressure oscillations are well captured by the ROM. Also in the region between the cylinder and the source, the acoustic field is recovered, however in the external part, for $x/R > L/R$, the agreement is very poor. The error is evident in the comparison of the SPL, in Figure 2-(b).

To improve the model, a more refined sampling has been made. With 17 snapshots in the interval $L/R = 1.5 \div 3.5$ with a step of 0.125. The comparisons between the high-fidelity and the ROM solutions are reported in Figures 3-(a,b). In this case the acoustic field along the line $y = 0$ is well represented by the ROM, also in the external part of the field ($x/R > L/R$), as shown by the comparison of the SPL. In Table 1 the values of the eigenvalues λ_l , $l = 1, 17$ and the corresponding value of $\varepsilon(l)$ defined by Equation (19). It is possible to remark that almost all the energy contents is already represented by the first mode. However, to recover, with a good degree of accuracy, the exact solution in the entire domain, it is necessary to retain most of the computed modes.

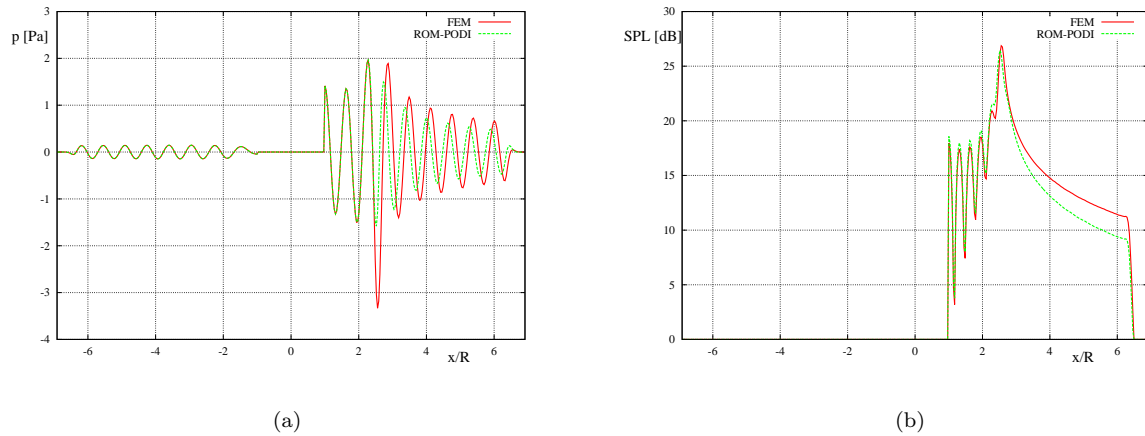


Figure 2. Scattering of a monopole acoustic source from a circular cylinder. $k = 10$, $L/R = 2.5625$. (a) Instantaneous pressure [Pa] and (b) SPL [dB], along the line $y = 0$, $k = 10$. Comparison of the PODI-ROM reconstruction (9 snapshots) with the numerical (FEM) solution.

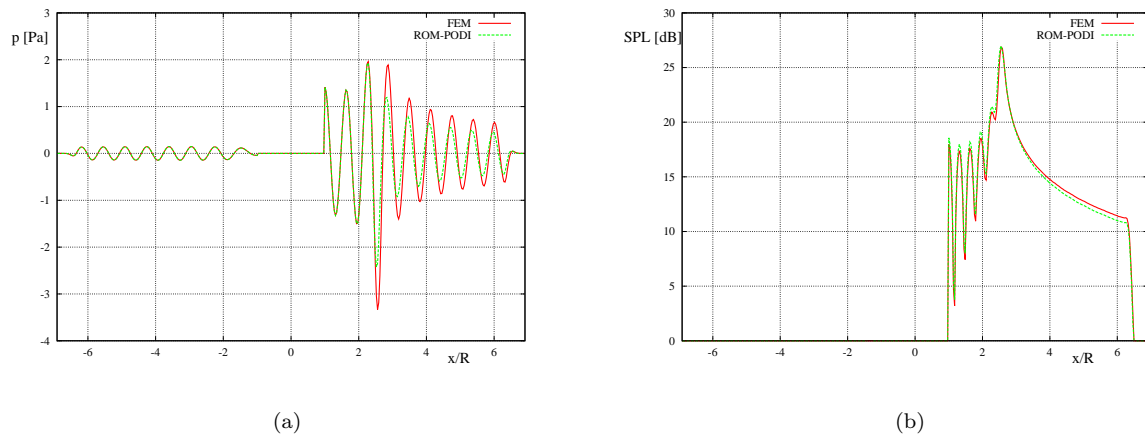


Figure 3. Scattering of a monopole acoustic source from a circular cylinder. $k = 10$, $L/R = 2.5625$. (a) Instantaneous pressure [Pa] and (b) SPL [dB], along the line $y = 0$, $k = 10$. Comparison of the PODI-ROM reconstruction (17 snapshots) with the numerical (FEM) solution.

V. Conclusions

A reduced-order model for acoustic propagation has been proposed. It is based on a Proper Orthogonal Decomposition of a set of high-fidelity calculations for different values of geometrical and frequency parameters of the acoustic problem. The POD expansion coefficients, functions of the parameters, were continuously extended in the parameter space by interpolation. This approach is termed POD with Interpolation (PODI). After these preliminary phase, which is performed offline, the ROM-PODI low-dimensional model can be used for rapid calculations, for example in the context of an optimization procedure. As a preliminary test, the ROM-PODI was applied to the case of the scattering of sound by a circular cylinder. The problem was formulated in the frequency space and the parameter was the distance of the monopole source with respect to the circular cylinder. The proposed methodology is able to correctly capture the main features of the acoustic field, such as the SPL field. Even if most of the energy contents is captured by the first modes, it has been shown that more modes are necessary in order to recover the exact field in all the domain.

Table 1.

l	λ_l	$(\sum_{i=1}^l \lambda_i / \sum_{i=1}^m \lambda_i) \times 100$
1	516113.17	94.81
2	19281.36	98.35
3	4219.60	99.13
4	1703.88	99.44
5	1161.57	99.65
6	679.12	99.78
7	402.54	99.85
8	271.58	99.90
9	170.02	99.93
10	111.85	99.95
11	81.05	99.969
12	56.53	99.9796
13	48.59	99.9886
14	27.27	99.9935
15	14.88	99.9963
16	12.48	99.9986
17	7.65	100.00

References

- ¹Kierkegaard, A., Boij, S. and Efraimsson, G., A frequency domain linearized Navier-Stokes Equations Approach to Acoustic Propagation in Flow Ducts with Sharp Edges, *The Journal of the Acoustical Society of America*, **127** (2), 710–719, (2010).
- ²Arina, R., Validation of a Discontinuous Galerkin Implementation of the Time-Domain Linearized NavierStokes Equations for Aeroacoustics, *Aerospace*, **3**, (7) doi:10.3390/aerospace3010007, (2016).
- ³Chinesta, F., Huerta, A., Rozza, G. and Willcox, K., Model Order Reduction, *Encyclopedia of Computational Mechanics*, Wiley, (2016).
- ⁴Rowley, C. W., Colonius, T. and Murray, R. M., Model Reduction fo Compressible Flows Using POD and Galerkin Projection, *Physica D*, **189**, 115–129, (2004).
- ⁵Epureanu, B. I., A Parametric Analysis of Reduced Order Models of Viscous Flows in Turbomachinery, *J. of Fluids and Structures*, **17**, 971–982, (2003).
- ⁶Legresley, P. A. and Alonso, J. J., Airfoil Design Optimization Using Reduced Order Models Based on Proper Orthogonal Decomposition, AIAA 2000-2545, *Fluids 2000 Conference*, Denver, Colorado, June (2000).
- ⁷Bui-Thanh, T., Damodaran, M. and Willcox, K., Aerodynamic Data Reconstruction and Inverse Design Using Proper Orthogonal Decomposition, *AIAA Journal*, **42** (8), 1505–1516, (2004).
- ⁸Mifsud, M. J., Shaw, S. T. and MacManus, D. G., A High-fidelity Low-cost Aerodynamic Model Using Proper Orthogonal Decomposition, *Int. J. Numer. Meth. Fluids*, **63**, 468–494, (2010).
- ⁹Tang, L. and Shyy, W., Proper Orthogonal Decomposition and Response Surface Method for TPS/RLV Structural Design and Optimization: X-34 Case Study, AIAA 2005-0839, *43rd AIAA Aerospace Sciences Meeting*, Reno, Nevada, January (2005).
- ¹⁰Lario, A. and Arina, R., Linearized Navier-Stokes Equations and their Numerical Solution, *22nd AIAA/CEAS Aeroacoustics Conference; Lyon, France*, AIAA Paper 2016-2973, (2016).
- ¹¹Lumley, J. L., The Structures of Inhomogeneous Turbulent Flows, *Atmospheric turbulence and radio propagation*, Yaglom, A. M. and Tatarski, V. I. ed.s, 166-178, Nauka, Moscow, (1967).
- ¹²Lumley, J. L., *Stochastic Tools in Turbulence*, Academic Press, New York, (1970).
- ¹³Loève, M., *Probability Theory*, D. Van Nostrand Company Inc., New York, (1955).
- ¹⁴Hotelling, H., Analysis of a Complex of Statistical Variables with Principal Components, *Journal of Educational Psychology*, **24**, 417-441, (1933).
- ¹⁵Liang, Y. C., Lee, H. P., Lim, S. P., Lin, W. Z. and Lee, K. H., Proper Orthogonal Decomposition and its Applications - Part I: Theory, *J. Sound and Vibration*, **252** (3), 527–544, (2002).
- ¹⁶Thomas, J. P., Dowell, E. H. and Hall, K. C., Three-Dimensional Transonic Aeroelasticity Using Proper Ortogonal Decomposition-Based Reduced-Order Models, *J. of Aircraft*, textbf40, (3), 544-551, (2003).
- ¹⁷Kim, T., Frequency-Domain Karhunen-Loeve Method and Its Application to Linear Dynamic Systems, *AIAA Journal*,

36, pp. 2117-2123, (1998).

¹⁸Volkwein, S., Proper Orthogonal Decomposition: Theory and Reduced-Order Modelling, Tech. Notes, University of Konstanz, Konstanz, Germany, <http://www.math.uni-konstanz.de/numerik/personen/volkwein/teaching/POD-Vorlesung.pdf>, (2013).

¹⁹Sirovich, L., Turbulence and the Dynamics of Coherent Structures, Part 1: Coherent Structures, *Quarterly of Applied Mathematics*, **45**, (3), 561-590, (1987).

²⁰Myers, R. H., Montgomery, D. C. and Anderson-Cook, C. M., *Response Surface Methodology*, 3rd ed., Wiley, New York, (2009).

²¹Hecht, F., New Developments in FreeFem++, *J. Numer. Math.*, **20** (3-4), 251-265, (2012).

²²Morris, P.J., The Scattering of Sound from a Spatially Distributed Axisymmetric Cylindrical Source by a Circular Cylinder, *J. Acoust. Soc. Am.*, **97** (5), 2651-2656 (1995).

²³Harari, I., Slavutin, M. and Turkel, E., Analytical and Numerical Studies of a Finite Element PML for the Helmholtz Equation, *J. Comput. Acoustics*, **8** (1), 121-137, (2000).